Optimisation of beam optics in the Van de Graaff accelerator microbeam at iThemba LABS and its Results on the Biomedical Analysis

M.E.M. Eisa[1, 2*], C.A. Pineda-Vargas[2,3] , A.L. Rodger [4], J.L . Conradie[5]

[1]Sudan University of Science and Technology, Department of Physics, P.O. Box 407, Post Code 11113, Khartoum, Sudan
[2]Materials Research Group, iThemba LABS, 7129Somerset West, South Africa
[3]Groote Schuur Hospital, Private Bag, Observatory 7935, South Africa
[4]Dep. of Chemistry, University of Cape Town, Private Bag, Rondebosch, South Africa
[5]Accelerator Group, iThemba LABS, P.O. Box 722, Somerset West 7129, South Africaca

PACS: 41.85.-p; 42.62.Be

Keywords: Van de Graaff; Beam optics; Nuclear Microprobe, PIXE

* Email contact of main author: memeisa@yahoo.com

Abstract. To improve the beam quality and intensity of the Van de Graaff accelerator at iThemba LABS, it is important to know the beam optics from the ion source. The ion source characteristics and optimal operating conditions were determined on an ion source test bench. The results of microbeam obtained with different computer codes are compared and discussed. The capabilities of the nuclear microprobe facility were evaluated in the improved beamline, with particular emphasis to bio-medical samples such as human hair, kidney stones and teeth. As a result of these improvement applications of PIXE and RBS techniques performed and this showed significant sensitivity. As well measurements carried out to compare elemental content and spatial distribution within two distinct human population groups, and to assess possible similarities and/or differences, hair samples from Sudan and South Africa were collected. Proton backscattering and Micro-PIXE were used to determine the matrix composition and content of light and middle transition elements. Mapping analysis showed a relatively similar content distribution for S, Cl, K and Ca within each group. However significant differences, particularly for heavier metals, such as Fe and Zn were also found.

1. Introduction

The beam quality and intensity have not been sufficient for high-resolution Ion Beam Analysis (IBA) and in particular Nuclear Microprobe (NMP) work. Previous studies have shown that ion source stability and efficiency is the most important factor to ensure a reliable beam probe at the NMP target surface [1,2]. Major efforts have been made recently to improve the reliability of this accelerator [3]. One important aspect was a thorough study of the beam optics from the ion source through the accelerator in order to understand the poor beam transmission at terminal voltages below 3 MV and also to find means of increasing the beam intensity delivered by the accelerator. Over a period of months it was found impossible to match the focusing condition of the beam at the exit of the accelerator to the admittance of the beam line, when using extraction voltages of more than 5 kV together with the original design of the electrodes configuration and power supplies. However, limiting the extraction voltage to less than 5 kV, has a great influence on the maximum beam current that can be obtained from the ion source and therefore on the beam intensity available from the accelerator. In order to understand this behavior and to find an ion optical solution for these conditions, the ion source was analysed in a test bench. Beam characteristics and profiles were calculated with the software programs TRANSPORT [4,5], IGUN [6] and TOSCA [7].

Details of the calculated beam optics as well as modifications to improve the transmission through the accelerator from the ion source to the analyzing magnet will be discussed.

2. Optimization of the beam current with extracting voltage

The solid lines in Fig. 1 show the measured beam current I_{beam} for different hydrogen ion species as a function of the extraction voltage U_{ex}. The remaining ion source parameters were kept at the following constant values: arc current I_{arc} = 1 A, arc voltage U_{arc} = 83 V, filament current I_{fil} = 25 A, pressure P = 10^{-5} mbar. The dotted lines in the figure are least-square fits of the Child-Langmuir equation (I_{beam} = constant × $U_{ex}^{3/2}$) to the measured data for the different ion species and show that the source behavior is to a large extent in agreement with the Child-Langmuir law. Furthermore, it indicates that the beam losses in the beam line due to space-charge effects are small and only of importance for operation at low extraction voltages as shown i (n see FIG.1.). For high beam intensity the source should be operated at the highest possible extraction voltage without jeopardizing reliability of beam delivery due sparking to

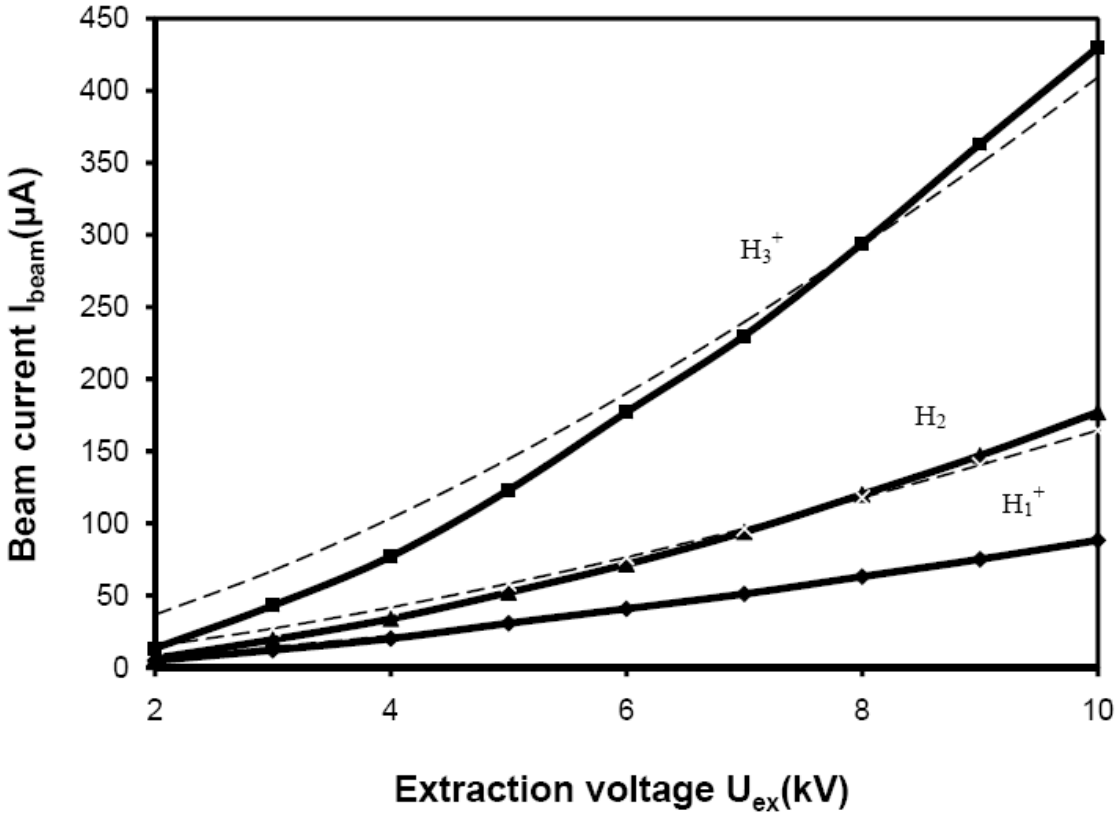

FIG. 1. Measured beam current (solid lines) for different Hydrogen ion species as a function of the extraction voltage, for the hot-cathode duoplasmatron ion source and least- square fits (dotted lines) of the Child-Langmuir law.

3. Biomedical Applications

3.1. Kidney Stones

A group of kidney concretions from the central regions of Sudan and eight from The Western regions of South Africa were considered for this investigation. Size of stones varied from small (~1-3 mm) to big (~1-3 cm). Their matrix composition (as determined by proton-BS, see Table 1). Clinically removed concretions were embedded in epoxy at room temperature. Cross sections through the core were cut with a diamond saw. The resulting flat surfaces were carbon coated prior to proton bombardment. Samples were irradiated at the NMP facility at the 6 MeV VDG accelerator of iThemba LABS [8,9] with 3 MeV protons. Beam currents of ~200-400 pA were used to ensure that no evaporation of constituents occurred due to possible rise in temperature generated at the probed sample volume (to a depth of ~100 μm). Micro-regions (~100-1000 μm) of interest were scanned by the 1-2 μm beam probe, at duel times of 10 ms, Scan size of 128 x 128 pixels were used to ensure a good resolution for mapping visualization. The Sudanese series was separated into two subgroups, characterized by high levels of Sr (sub-group 1) and Fe (sub-group 2). Two stones from Sudan 3A and 2B were found to be correlated with the South African group. Although the 2 subgroups (in Table 1) of stones from Sudan originated from two different regions within Sudan, the grouping as shown in Figure 2 does not appear to be associated to the geographical situation. On the contrary, Sudanese stones were grouped according to sub-groups 1 and 2 (see FIG. 2.). These two sub-groups contain Sudanese stones from both locations.

TABLE 1: KIDNEY TRACE ELEMENTAL CONCENTRATIONS AS DETERMINED BY μ-PIXE IN $\mu g.g^{-1}$. MAJOR COMPONENTS LEVELS ARE GIVEN AS ATOMIC RATIOS DETERMINED BY PROTON-BS. THE TYPICAL STANDARD DEVIATION ON PIXE DETERMINATION WAS ~5%.

	Micro-PIXE							Proton-BS			
	Fe	Cu	Zn	Se	Br	Sr	Sn	C	O	N	Ca
1	39	3.0	67	1.6	0.1	151	11	2	4		1
2	200	5.5	145	1.1	10.3	43	34	16	4	9	1
3	73	4.0	61	3.0	6.0	59	36	2	4		1
4	73	8.7	4.2	0.9	1.8	0.6	18	7	4	46	
6	185	3.3	50	1.4	4.8	9.1	17	3	4	3	
S1	532	10.0	51	0.1	13.0	52	60	6	4	1	1
S2	17	4.0	182	0.1	4.0	377	40		4	3	2
S3	205	2.6	755	3.1	22.8	143	26	5	4	1	1
S4	23	4.0	214	2.2	11.0	108	42	3	4		1
S5	312	2.6	73.5	0.7	7.0	10.2	11	7	4	60	
2117B	2	0.1	1.6	1.5	2.8	7	88	5	4	1	1
2240B	41	8.0	81	7.0	9.0	29	56	3	4		1
2243B	61	0.1	55	0.1	5.0	32	38	2	4	1	
2260B	45	4.0	27	0.1	3.8	16	31	8	4	46	
2287A	103	0.1	24	0.1	3.2	36	51	2	4	1	1
2302A	25	0.1	572	1.3	4.5	185	15	4	4		2
2336A	63	1.4	21	0.1	0.8	15.2	15	20	4	5	
UWE B	38	0.1	63	4.0	5.0	37	59	2	4	2	1

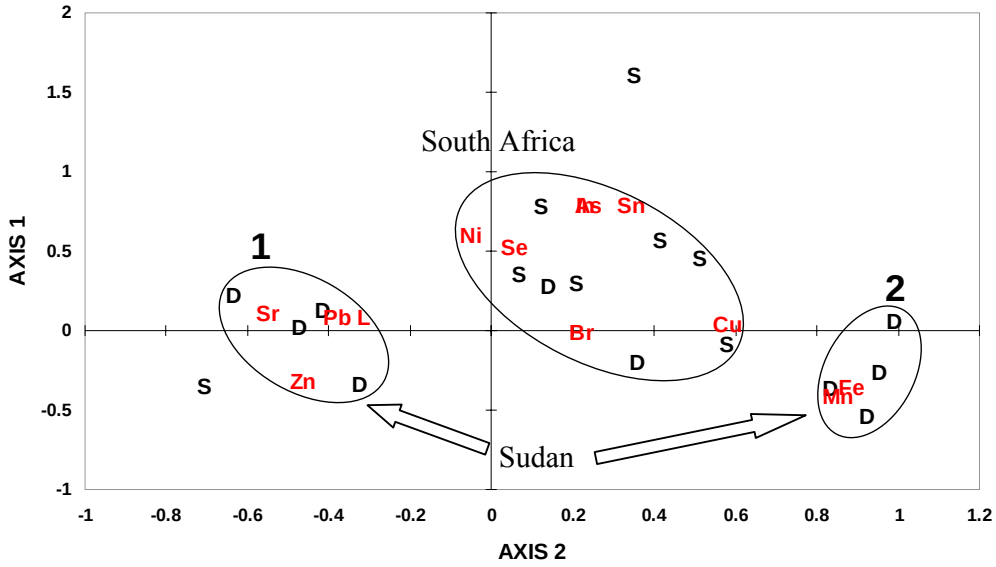

FIG. 2: Correspondence Analysis of the first two axes for the two groups of kidney stones from Sudan (D) and South Africa (S). Stones from South Africa are clearly clustered into one group. One outlier (S) has elemental profile that resembles mostly the group 1 from Sudan.

3.2. Teeth Elemental Mapping

Elemental quantitative maps for Sr and Zn to a lesser extent showed that their distribution levels over the area comprising the interface enamel-dentine were lower for the enamel. This applies particularly for specimens after erosion treatment. The depletion of Sr may act as a protectant to demineralization, contrary to the increase in certain elements such Fe and Ni. Although it's not clear why there appear to be a re-mineralisation process for these two elements it is envisaged that their role in erosion is not well understood. Figure 2 shows the mapping over an irradiated interface of a dentine control sample. The mapping correlation between Ca and Zn on the left of the figure clearly shows two kinds of correlation distributions, each associated with either the dentine or enamel area. The trend of the interface boundary is also visible. The weakest correlation corresponds to that of enamel. The correlation between Ca and Ni on the contrary exhibit mainly one strong correlation over the dentine area. In some elemental maps (i.e., Ni) the interface enamel-dentine was not well defined but it appeared as a wider band covering sections of the both the enamel and dentine areas with gradual variation of the corresponding mapped element. To assess these gradual linear variations, linear traverses were extracted from maps of selected elements. Figure 3 shows the map of Zn for the same dentine control sample shown in Figure 2. The area used for the traversed is plotted over the map. It was found that most elements exhibit gradual variations of depletion or enrichment when considering the direction from the enamel to the dentine (see FIG.3.). For example, Zn have a value of ~50 $\mu g.g^{-1}$ over the enamel region, its concentration level increase over the interface band to ~150$\mu g.g^{-1}$ in the direction to the dentine. Similar profile can be seeing for Ni and Cu. On the other hand Sr had an opposite behavior with lower values (~80$\mu g.g^{-1}$) in the dentine area. Previous results on the concentration profile of human teeth on the enamel-dentine interface showed similar trend for Sr [10].

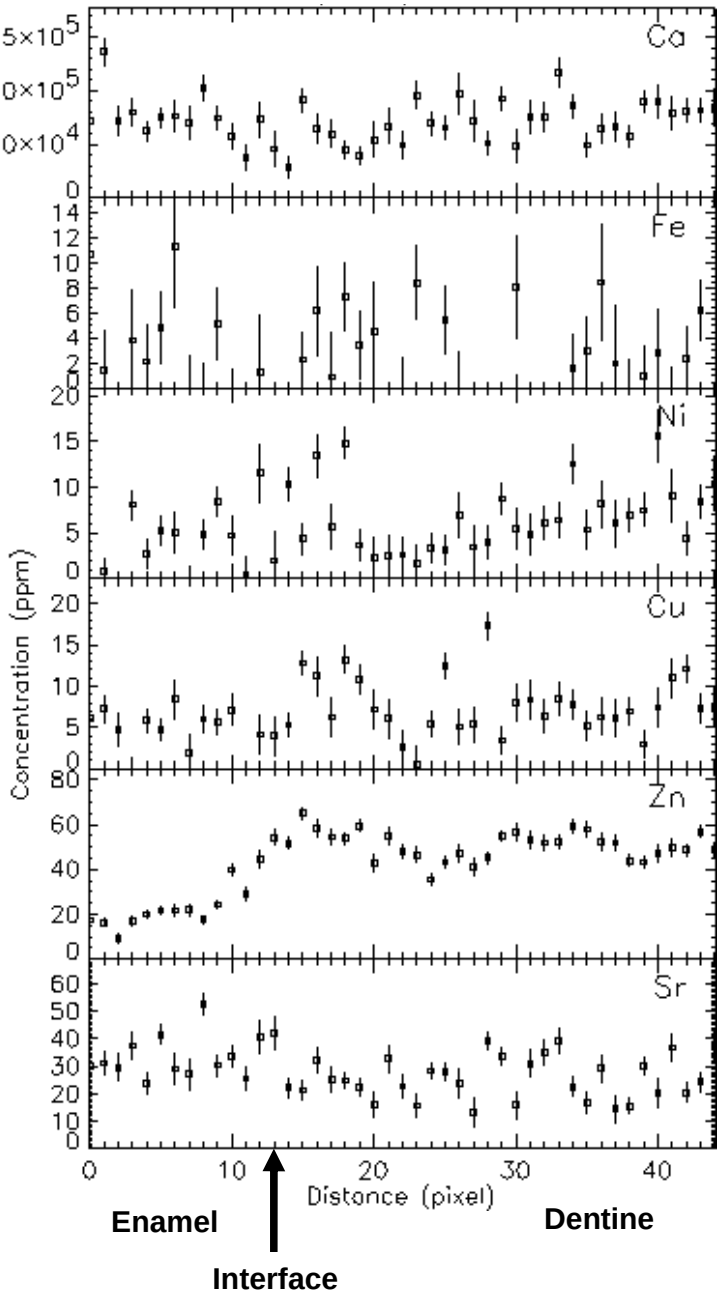

FIG. 3: The map of Zn for a dentine control sample over an irradiated area of ~1000 µm^2. The interface enamel-dentine is clearly visible. The box used to extract the traverse profile in Figure 4 is plotted over the map. Concentrations are given in µg.g^{-1}.

3.3. Human Hair Measurements by NMP

Hair Samples were irradiated at the Nuclear Microprobe (NMP) facility. More detailed description of the experimental set-up has been reported previously [8, 11]. Proton beams with energy of 1.5 and 3.0 MeV were selected for analysis of particular micro-regions of hair-shaft cross sections. Beam currents of ~50 pA were used to prevent evaporation of elements. Selected micro-regions were scanned with focused proton beam of 2 – 3 μm spot size, with resolution of 128 x 128 pixels and 10 ms dwell time. Elemental mapping of hair samples with 1.5 MeV protons were obtained by DA analysis. The distribution of certain elements such as S, K, Ca and Zn were clearly observed in the cuticle, cortex and medulla areas of the hair cross sections. FIG.4. shows the maps of S and Ca for a typical Sudanese samples and one of the South African samples. While sulphur is distributed similarly in both samples there appear to be an inverse correlation of the calcium content in the medulla area of the hair shaft. FIG.5. show maps of Ti and Zn obtained as well with irradiation with 1.5 MeV. In the Sudanese sample S1, Ti was enriched more in the cortex while in the South African sample SA2, it was equally distributed in both the medulla and the cortex.

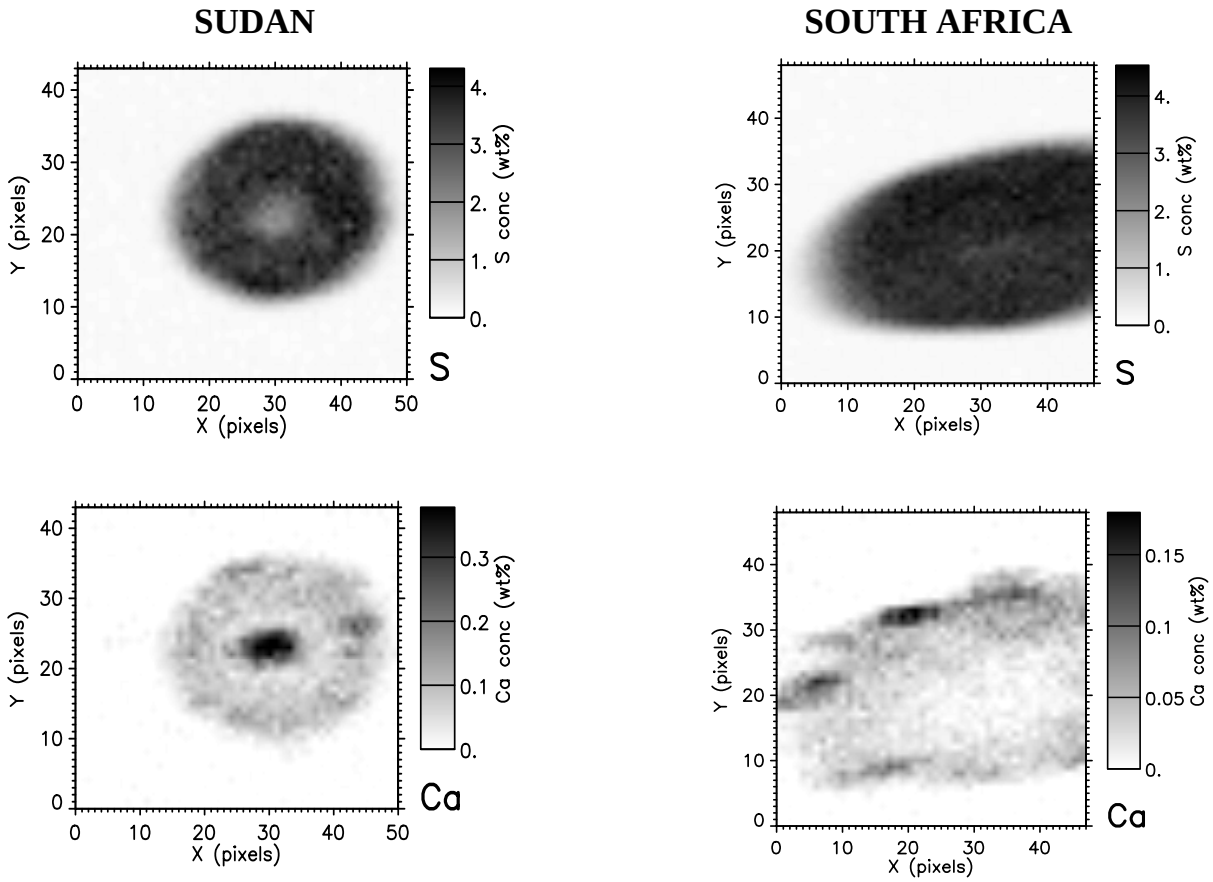

FIG. 4: Maps of sulphur and calcium for a typical Sudanese and South African samples. Note the inverse correlation of calcium content in the medulla. Sulphur appears to be distributed similarly in both samples

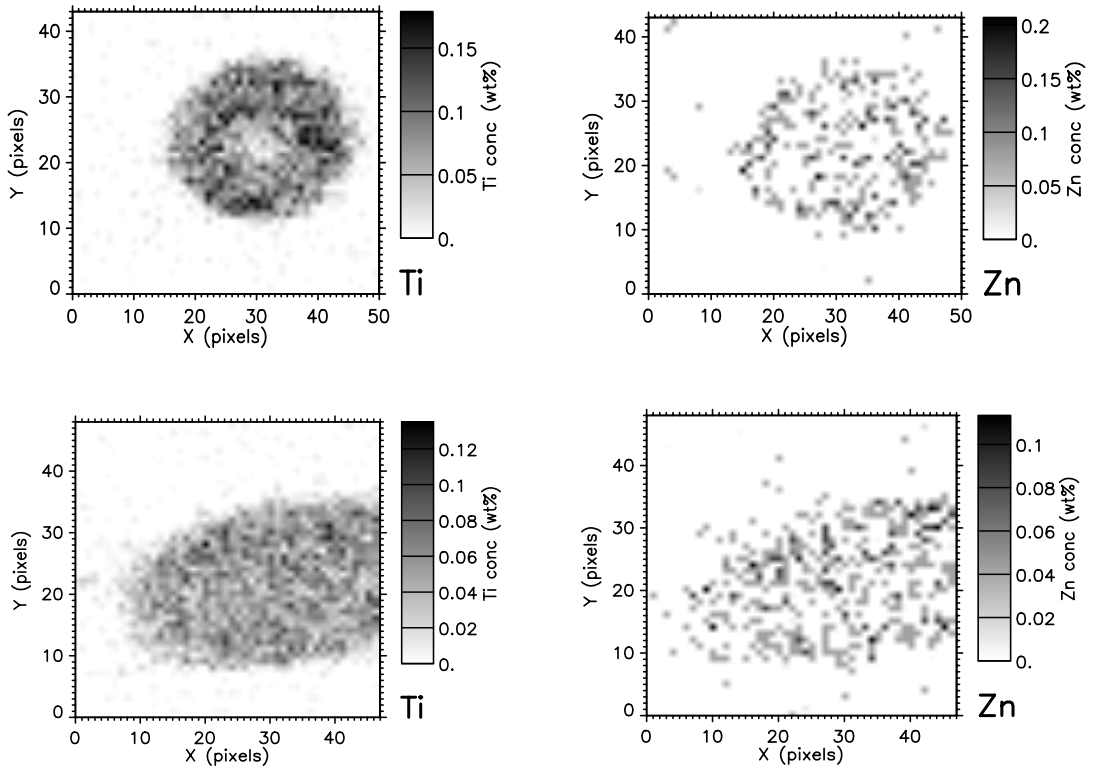

FIG. 5: Maps of titanium and zinc for a Sudanese (S1) and South African (SA2) samples. In the Sudanese sample S1, Ti is enriched more in the cortex while in SA2 Ti is equally distributed both in medulla and cortex.

4. Conclusion

Subsequent to the optimisation of beam optics, relevant applications of biomedical samples were measured to demonstrate the capabilities of the nuclear microprobe at iThemba LABS were undertaken with emphasis in the characterisation and spatial distribution of trace metals in hard human tissues such as kidney concretions, teeth enamel and hair cross sections which showing very sensitive change in the NMP after the beam optimisation. Information on the major components showed marked differences particularly for O, P and F. Analysis by μ-PIXE showed that the levels of trace elements were enriched or depleted according to the type of erosion treatment. Mapping comparison showed that the structure of dentine and enamel is not uniform with respect to the spatial distribution of trace elements and this may determine the cause of teeth demineralization processes exposed to acidic media.

Two groups of human kidney concretions from South Africa and Sudan were compared in terms of their matrix-composition as determined by μ-PIXE and proton-BS. The concentration values of the trace elements analysed by (Fe, Cu, Zn, Se, Br and Sr) showed a linear trend when their mean was plotted for both groups of stones. Statistical analysis of μ-PIXE data evaluated by correspondence analysis showed the formation of two clusters, corresponding to each the South African and the Sudanese stone groups.

In the hair samples the main objective was to compare element content and spatial distribution within scalp hair-shaft cross sections of this two distinct human population groups, and to assess possible similarities and/or differences. Mapping analysis showed a relatively similar content distribution for K and Ca within each group. However significant differences, particularly for heavier metals, such as Ti and Zn were also found.

References

[1] Grime G.W. and Watt F., Nucl. Instr. and Meth. B30 (1988) 227.
[2] Kalbitzer, S., Nucl. Instr. and Meth. B158 (1999) 53.
[3] Pineda-Vargas, C.A., Eisa, M.E, Chikte, U.M.E., Conradie, J.L., Radiation Physics and Chemistry 71 (2004) 937.
[4] Carey, D.C., The Optics of Charged Particle Beams, Harwood Academic Publishers, London, 1987.
[5] Carey, D.C., Nucl. Instr. and Meth. 187(1972) 173.
[6] Becker, R., New features in the Simulation of Ion Extraction with IGUN, Proceedings of the 6th European Particle Accelerator Conference, Stockholm, June 1998, 1165.
[7] Borburgh, J., 2-Dimensional Finite Element Calculations on a Septum Magnet with Opera2D, CERN Note PS/CA/Note 97-27.
[8] Prozesky, V.M., Przybylowicz, W.J., Van Achterbergh, E., Churms, C.L., Pineda, C.A., Springhorn, K., Pilcher, J.V., Ryan, C.G., Kritzinger, Schmitt, J.H., Swart. T., The NAC nuclear microprobe facility. Nucl. Instr. and Meth. B104(1995) 36-42.
[9] Przybylowicz, W.J., Mesjasz-Przybylowicz, J., Pineda, C.A., Churms, C.L., Ryan, C.G., Prozesky, V.M., Frei, R., Slabbert, J.P., Padayachee J., Reimold, W.U.,2001
[10] Pinheiro, T., Carvalho M.L., Casaca, C., Barreiros, M.A., Cunha, A.S., Chevallier, P., 1999. Microprobe analysis of teeth by synchrotron radiation: environmental contamination, Nucl. Instr. And Meth. B 158, 393-398.
[11] Przybylowicz, W.J., Mesjasz-Przybylowicz, J., Pineda, C.A., Churms, C.L., Ryan C.G., Prozesky, V.M., Frei, R., Slabbert, J.P., Padayachee, J. and Reimold, W.U., X-ray Spectrometry, 30 (2001) 156.